

Supporting Information

Fast pseudocapacitive reactions of three-dimensional manganese dioxide structures synthesized *via* self-limited redox deposition on microwave-expanded graphite oxide

Wencong Zeng,^a Yuan Zhao,^a Kun Ni,^a Yanwu Zhu^{a,b,*}

^a *Key Laboratory of Materials for Energy Conversion, Chinese Academy of Sciences,*

Department of Materials Science and Engineering, University of Science and

Technology of China, Hefei, Anhui 230026, P. R. China

^b *iChEM (Collaborative Innovation Center of Chemistry for Energy Materials),*

University of Science and Technology of China, Hefei, Anhui 230026, P. R. China

*Corresponding author. E-mail address: zhuyanwu@ustc.edu.cn

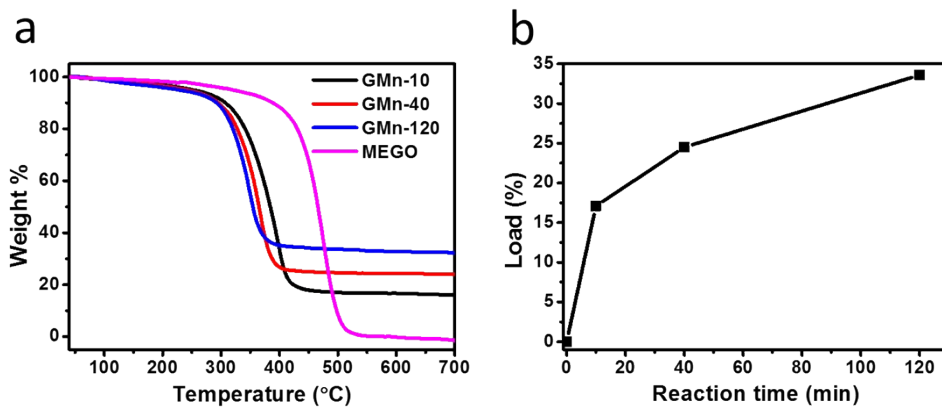


Fig. S1 (a) Thermogravimetric analysis of MEGO and MEGO–MnO₂ composites. (b) MnO₂ loading dependence on reaction duration.

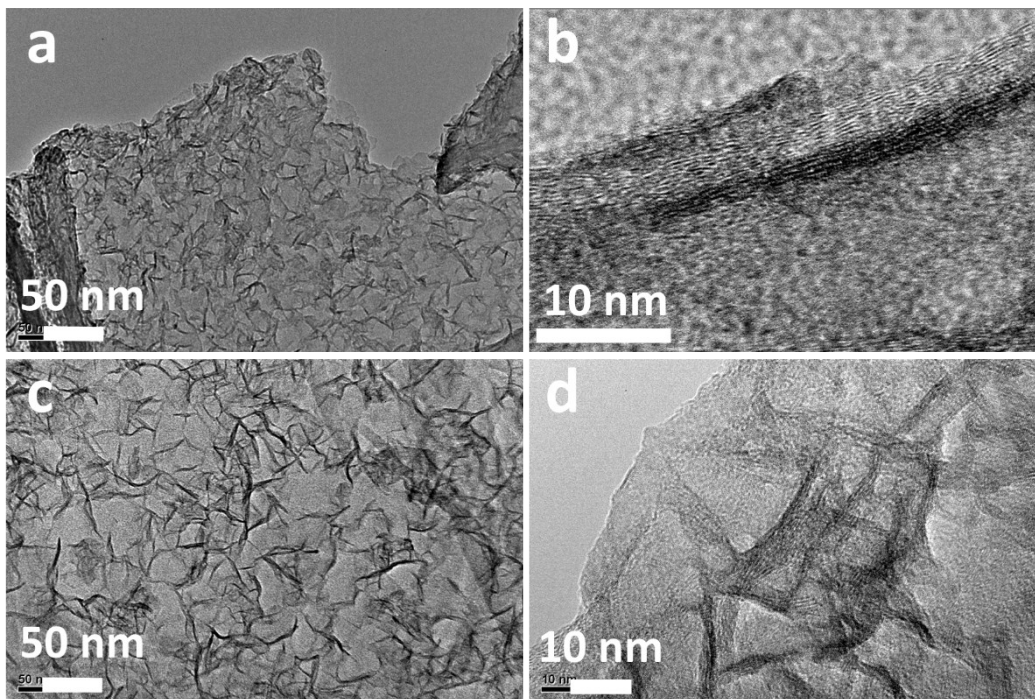


Fig. S2 TEM images of (a, b) GMn-10 and (c, d) GMn-120.

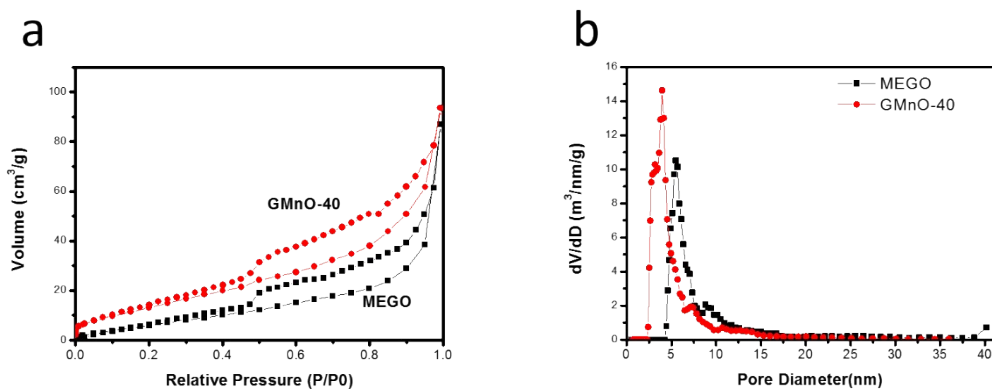


Fig. S3 (a) Nitrogen adsorption and desorption isotherms of MEGO and GMn-40. (b) Pore size distributions of MEGO and GMn-40.

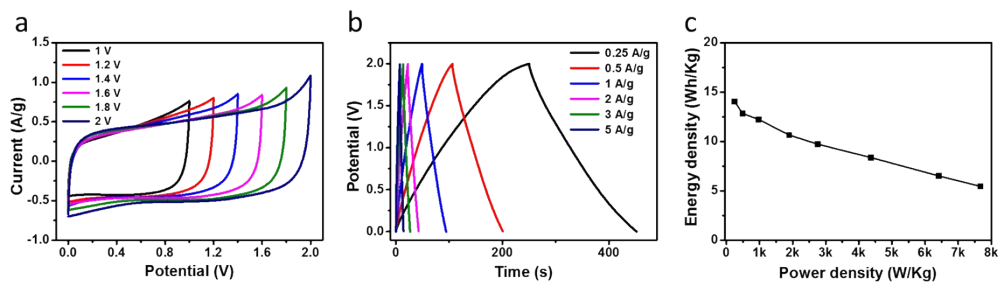


Fig. S4 (a) CV curves of a GMn-40 symmetric SC measured in various potential windows at a scan rate of 20 mV/s. (b) Galvanostatic charge–discharge curves obtained at various current densities. (c) Energy density versus power density for symmetric SCs based on GMn-40.

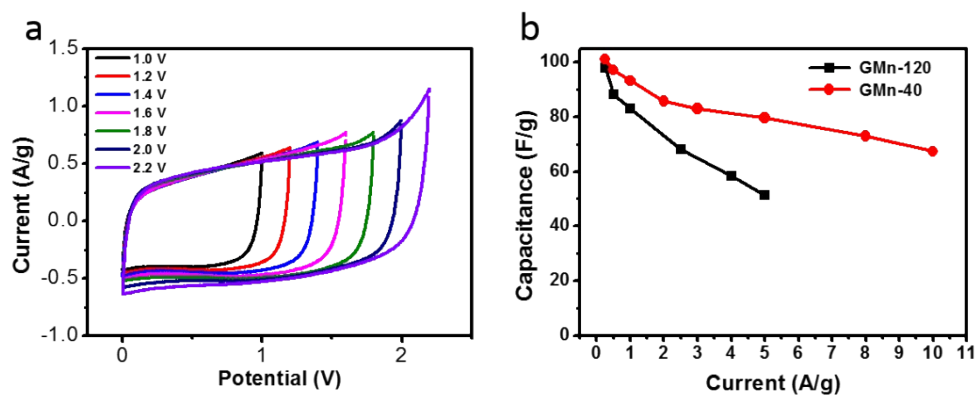


Fig. S5 (a) CV curves of a GMn-120 symmetric SC measured in various potential windows at a scan rate of 20 mV/s. It shows that the operating voltage of the SC was limited to ~ 2 V. (b) Specific capacitance of GMn-40 and GMn-120 symmetric SCs versus charge–discharge current density at a working potential of 2 V.

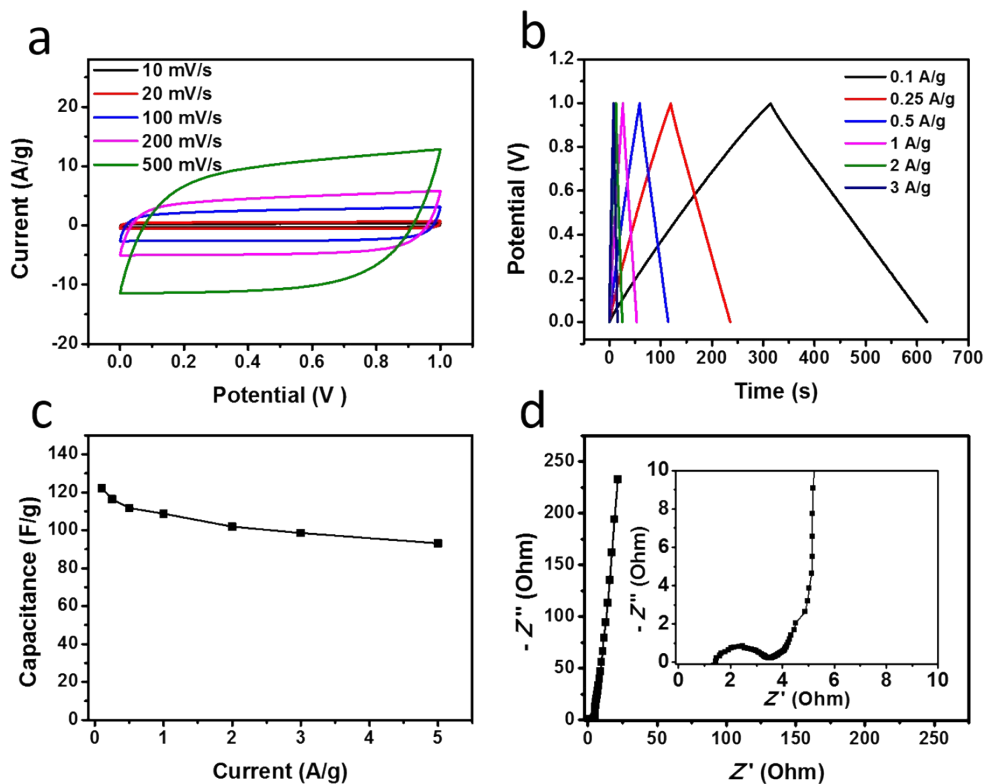


Fig. S6 (a) CV curves of an aMEGO symmetric SC in 1 M Na₂SO₄, measured at various scan rates. (b) Galvanostatic charge–discharge curves at different current densities. (c) Specific capacitances calculated from discharge curves. (d) Nyquist plot.

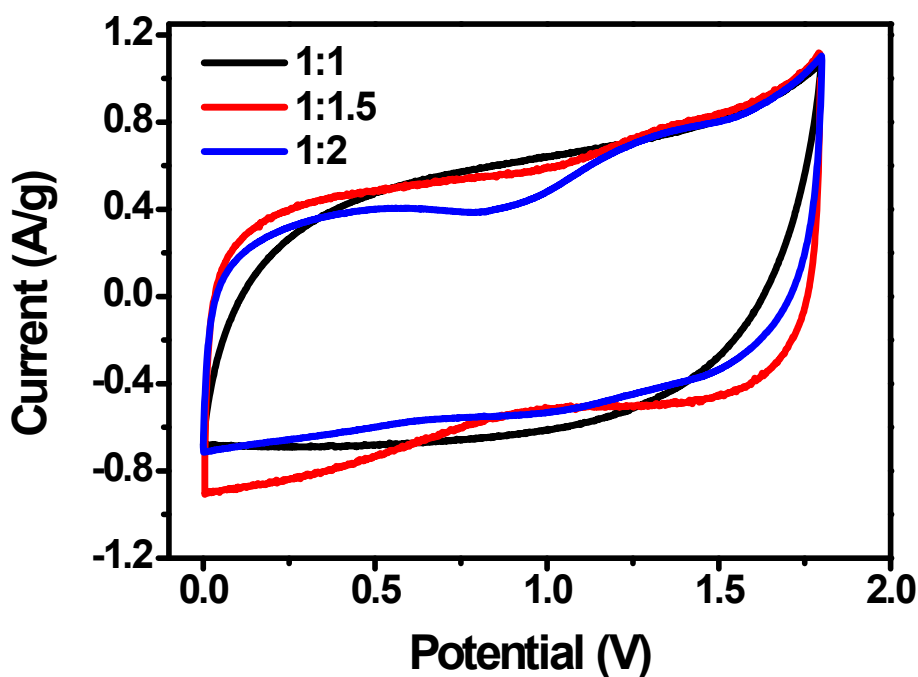


Fig. S7 CV curves of GMn-40//aMEGO asymmetric supercapacitors (with different mass ratios between the positive and negative electrodes) at 20 mV/s. The specific capacitance was 26, 29.3, and 24.9 F/g for an asymmetric SC with a mass ratio of 1:1, 1:1.5, and 1:2, respectively. These values were calculated from CV curves according to the equation $C_{cell} = (\int I dV)/(2vmV)$, where C_{cell} is the specific capacitance of an asymmetric SC (F/g), I is the response current (A), V is the potential (V), v is the scan rate (V/s), and m is the mass of two electrodes (g).

Table S1 I_D/I_G of MEGO and MEGO–MnO₂ composites calculated from Raman spectra.

	Position (cm ⁻¹)		Intensity (arb. unit)		I_D/I_G
	D band	G band	D band	G band	
MEGO	1362	1593	1883	1967	0.957
GMn-10	1356	1597	2475	2675	0.926
GMn-40	1350	1599	2426	2565	0.946
GMn-120	1357	1593	2165	2309	0.938

Table S2. Comparison of capacitive performance of the supercapacitors based on various MnO₂-based asymmetric presented in literature and the present work.

Supercapacitors structure	Method	Electrolyte	Operation voltage [V]	E(Wh/kg)	Ref
MnO ₂ -carbon paper// MnO ₂ -carbon paper	Chemical precipitation	1.0 M Na ₂ SO ₄ aqueous electrolyte	0.7 V	20.8	[1]
MnO ₂ Nanotubes//AG	Chemical precipitation	1 M Na ₂ SO ₄	1.8 V	22.5	[2]
CuO@MnO ₂ //MEGO	Chemical precipitation	1 M Na ₂ SO ₄	1.8 V	22.1	[3]
Graphene-Patched CNT-MnO ₂ //CNT-PANI	Galvanostatic electrochemical deposition	1 M Na ₂ SO ₄ - PVP gel	1.6 V	24.8	[4]
GMN-40//aMEGO	Chemical precipitation	1 M Na ₂ SO ₄	1.8 V	25.1	This work

References:

- 1 S. J. He, C. X. Hu, H. Q. Hou and W. Chen, *J. Power Sources*, 2014, **246**, 754.
- 2 M. Huang, Y. X. Zhang, F. Li, L. L. Zhang, R. S. Ruoff, Z. Y. Wen and Q. Liu, *Sci. Rep.*, 2014, **4**; DOI:10.1038/srep03878.
- 3 M. Huang, Y. X. Zhang, F. Li, Z. C. Wang, Alamusi, N. Hu, Z. Y. Wen and Q. Liu, *Sci. Rep.*, 2014, **4**; DOI:10.1038/srep04518.
- 4 Y. Jin, H. Y. Chen, M. H. Chen, N. Liu and Q. W. Li, *ACS Appl. Mater. Interfaces*, 2013, **5**, 3408.